External high quality-factor resonator tunes up nuclear magnetic resonance: Supplementary information

Stephan Appelt[1,2*], Martin Suefke[3], Alexander Liebisch[2], and Bernhard Blümich[2]

[1]*Central Institute for Engineering, Electronics and Analytics – Electronic Systems (ZEA-2), Forschungszentrum Jülich GmbH, D-52425 Jülich, Germany.*

[2]*Institut für Technische Chemie und Makromolekulare Chemie (ITMC), RWTH Aachen University, D-52056 Aachen, Germany.*

[3]*Institute of Energy and Climate Research – Fundamental Electrochemistry (IEK-9), Forschungszentrum Jülich GmbH, D-52425 Jülich, Germany.*

[*]*e-mail: st.appelt.@fz-juelich.de*

I. Abragam's formulation of *SNR*

The theoretical considerations begin by inspecting Abragam's [1] formula for the *SNR* of magnetic resonance detected with a standard *LC* resonance circuit at the frequency $\omega_0 = 2\pi\nu_0$. Given the quality factor of the input coil $Q = \omega_0 L/R$, the sample volume V, the magnetization $M_0 = \chi_0 H_0$, (χ_0: magnetic susceptibility, H_0: magnetic field) and the detection bandwidth $\Delta\nu$, then the *SNR* is given by

$$SNR = k_0 \sqrt{\frac{\mu_0}{4}\frac{2\pi\nu_0}{\Delta\nu} Q\ \chi_0 \frac{H_0 M_0 V}{k_B T}} \quad \text{(S1)}.$$

The constants μ_0 and k_0 are the vacuum permeability and a factor describing the B_1 field homogeneity of the coil ($k_0 \sim 1$ for a homogeneous B_1 field), respectively. In Eq. S1, the square root of *SNR* is proportional to $Q^{1/2}$ and to the ratio between the magnetic energy

$H_0 M_0 V_s$ of the nuclear spins and the thermal energy $k_B T$ of the coil. For a cylindrical and symmetrical thin coil (inner diameter D_i = height H) with n turns and inductivity $L = \mu_0 \pi n^2 D_i/4$, Eq. S1 can be rewritten in a form which depends directly on the coil parameters Q, L, n, D_i and which can be compared to EHQE theory, as discussed later. By assuming $V = \pi D_i^2 H/4 = \pi D_i^3/4$, that the sample volume fits exactly into the cylindrical coil, and the detection bandwidth $\Delta\nu = \omega_0/(2\pi Q)$, Eq. S1 becomes

$$SNR = \frac{\pi^{3/2}}{8\sqrt{k_B T}} \frac{Q}{\sqrt{L}} k_0 \mu_0 M_0 D_i^2 n \quad \text{(S2)}.$$

If the coil volume shrinks in the same proportion as the sample volume V, then Eq. S2 simply reduces to $SNR \sim Q M_0 D_i^{3/2} \sim Q M_0 V^{1/2}$. Thus, the SNR does not depend on n but rather depends on the square root of V.

II. Signal and noise model for EHQE-NMR

Figure S1 shows the essential parts of the EHQE resonance circuit consisting of a thick cylindrical input coil with its geometrical parameters $D_i = H$, outer diameter D_a, number of turns n, number of turns per layer $W = H/d$ (d = wire diameter), a transfer line, a tuning capacitor C, an external inductivity with a high Q-factor, and a differential amplifier whose voltage and current noises are denoted as e_n and i_n, respectively. The electrical properties of the input coil are given by the inductivity L, the AC resistance R, and the quality factor $Q = \omega L/R$, and those of the external coil are L_E, R_E, and $Q_E = \omega L_E/R_E$, respectively. It is assumed that the AC resistance of the transfer line is small (however, it can be included as a small additional term in R) and that the Q-factor of the tuning capacitor $Q_C \sim 10000 > Q$. Both the current noise (i_n) and the voltage noise (e_n) of the differential amplifier are not yet neglected.

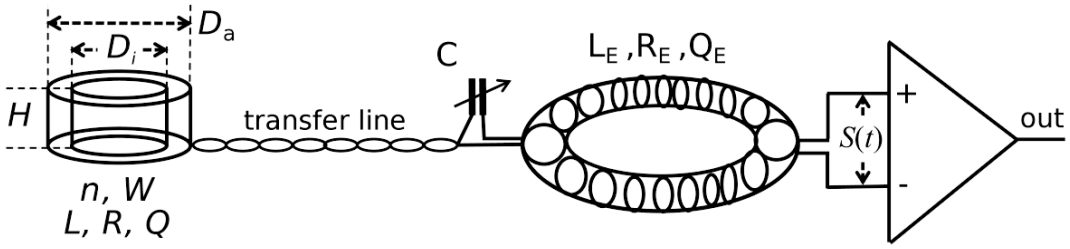

Fig. S1: Main parts of the EHQE-NMR resonance circuit. Not shown are the static magnetic field B_0, the excitation coil (saddle coil), and the sample with volume $V = \pi D_i^2 H/4$ located inside the input coil. After rf excitation, the precessing nuclear spins (Larmor frequency $\omega_0/2\pi = \gamma B_0$) of the sample induce an AC voltage given by $U_i = k_0 M_0 V (B_1/i) \omega_0$.

According to the principle of reciprocity [2], the voltage which is induced in the input coil by a precessing nuclear spin ensemble is given by $U_i = k_0 M_0 V (B_1/i)\omega_0$, where B_1/i (field per unit current) is the sensitivity of the input coil. The voltage $S(t)$ which is measured across L_E and which is fed into the input of the differential amplifier is given by $S(t) = L_E\, dI(t)/dt$, where $I(t)$ is the AC current flowing in the EHQE circuit. The term $I(t)$ can be derived by applying Kirchoff's second law to all components of Fig. S1 resulting in a first-order differential equation $L_{tot}\, dI(t)/dt + R_{tot}\, I(t) + C^{-1} \int I(t')dt' = U_i$. The total inductance and resistance is given by $L_{tot} = L + L_E$ and $R_{tot} = R + R_E$, respectively. After differentiation of this first-order equation with respect to t and division by L_{tot}, we obtain a second-order differential equation with an inhomogeneous source term proportional to U_i :

$$\frac{d^2 I(t)}{dt^2} + \frac{R+R_E}{L+L_E}\frac{d\,I(t)}{dt} + \frac{I(t)}{(L+L_E)C} = \frac{i\,\omega_0\, k_0\, M_0 V (B_1/i)\,\omega_0}{L+L_E} \exp(i\,\omega_0 t) \quad (S3).$$

Inspection of the particular solution of Eq. S3 with the ansatz $I(t) = I_0 \exp(i\omega t)$ leads to the result that a maximum current $I_0^{max} \exp(i\omega t)$ flows in the circuit if the resonance condition $\omega = \omega_0 = (L_{tot}\, C)^{-1/2}$ is fulfilled. At resonance, the maximal signal voltage $S_{max}(t) = L_E\, dI_0^{max}/dt$ is given by

$$S_{max}(t) = \frac{i\,\omega_0 L_E\, k_0\, M_0 V (B_1/i)\,\omega_0}{R+R_E} \exp(i\,\omega_0 t) = \frac{i Q_E\, k_0\, M_0 V (B_1/i)\,\omega_0}{1+R/R_E} \exp(i\,\omega_0 t) \quad (S4).$$

The factor $Q_E/(1+R/R_E)$ on the right-hand side of Eq. S4 is equal to Q_{red}, which is the reduced quality factor and describes the enhancement of the NMR signal induced in the input coil. The total noise measured at the bandwidth $\Delta\nu$ including Johnson noise of the input coil, voltage, and current noise (e_n, i_n) of the differential amplifier is given by

$$N = \sqrt{\left[e_n^2 + \left(R_{tot}\, Q_{tot}^2 \right)^2 i_n^2 + 4 k_B T\, R_{tot}\, Q_{tot}^2 \right] \Delta\nu} \quad \text{(S5)}.$$

The term $Q_{tot} = \omega L_{tot}/R_{tot}$ describes the total quality factor of the resonance circuit and $R_{tot} \cdot Q^2_{tot}$ is the total impedance seen at the input of the differential amplifier. For an EHQE resonator with high values of $Q_E >> 100$ and with $Q_{tot} \sim 300$, the impedance $R_{tot} \cdot Q^2_{tot}$ in resonance is typically in the megohm range so that the voltage noise e_n in Eq. S5 (typically a few nV/Hz$^{1/2}$) can be neglected. Some FET differential amplifiers operating in the lower frequency regime (1–500 kHz) have a current noise $i_n < 10$ fA/Hz$^{1/2}$ so that $4k_B T\, R_{tot}\, Q_{tot}^2 > R_{tot}\, Q^2_{tot}\, i_n$. Thus, the current noise term can also be neglected. Assuming that the detection bandwidth is dominated by the width of the EHQE bandpass curve which has a bandwidth of $\Delta\nu = \omega_0/(2\pi\, Q_{tot})$, then the noise term in Eq. S5 is reduced to $N = ((2/\pi)\, k_B T\, R_{tot}\, Q_{tot}\, \omega_0)^{1/2}$ which is equivalent to

$$N = \sqrt{2/\pi}\, \omega_0 \sqrt{k_B T \left(L + L_E \right)} \quad \text{(S6)}.$$

III. Model for a thick cylindrical input coil

Since most experimental results were obtained using thick cylindrical input coils with many turns $n >> 10$, the standard expressions for the inductivity L, the AC resistance R, and the sensitivity B_1/i for a thin cylindrical coil [2] (condition: $D_a - D_i << D_i$) do not work. For a thick coil, an extended model for L, R, and B_1/i is needed. According to Hoult and Richards [2], the sensitivity of a thin cylindrical coil with height H, diameter D_i, and number of turns n is given by $B_1/i = \mu_0\, n\, /(D_i^2 + H^2)^{1/2}$. We characterized a thick cylindrical coil (with

$H = D_i$) made of n turns of copper wire with diameter d by the number of turns per thin layer $W = H/d$, the number of complete thin layers k_{max} = Integer(n / W) and by the rest $n_{rest} = n$ modulo W of turns forming an incomplete layer at the maximum outer diameter $D_i + (k_{max}+1)$ d. Summing over all thin layers results in the exact expression for the total sensitivity of the thick coil

$$\frac{B_1}{i} = \frac{\mu_0}{D_i}\left(\left(\sum_{k=1}^{k_{max}} \frac{W}{\sqrt{2 + 2W^{-1}k + W^{-2}k^2}}\right) + \frac{n_{rest}}{\sqrt{2 + 2(k_{max}+1)W^{-1} + (k_{max}+1)^2 W^{-2}}}\right) \quad \text{(S7)}.$$

A Taylor series expansion of this expression in the parameter k / W << 1 in Eq. S7 up to the third order in n and neglecting the term containing n_{rest} results in

$$\frac{B_1}{i} = \frac{\mu_0}{\sqrt{2}\,D_i}\left(n - \frac{n^2}{4W^2} + \frac{n^3}{24W^4} + O\left(n^4\right)\right) \quad \text{(S8)}.$$

Eq. S8 is accurate enough within the boundaries of our experiments $W > 20$ and $n < 1000$. In analogy, by summing over all layers from $k = 1$ up to k_{max}, the inductivity L of a thick cylindrical coil is given by

$$L = \frac{\pi}{6}\mu_0 n^2 D_i\left(1 + \frac{n}{W^2}\right)^2 \quad \text{(S9)}.$$

Likewise, the AC resistance R including the skin and proximity effects is

$$R = \frac{4\rho D_i n}{d^2}\left[\left(1 + \frac{1}{2W}\right) + \frac{n}{2W^2}\right]\{Skin + Prox\} \quad \text{(S10)},$$

where ρ denotes the specific electrical resistance of the wire. The factor $(1 + n/W^2)^2$ in Eq. S9 and the terms containing W in the square bracket of Eq. S10 both account for the increasing enclosed area and length of the wire due to the increasing diameter of the thick input coil. The term in the square bracket including the prefactors in Eq. S10 describes the DC resistance of the thick input coil. The skin and proximity effects in Eq. S10 are abbreviated as *Skin* and *Prox* and represent the main AC loss factors in the copper wire. According to [3], these two

loss factors can be expressed as $Skin = 0.5\ \xi((\sinh \xi + \sin\ \xi)/(\cosh\ \xi\ -\ \cos\ \xi))$ and $Prox = (2/3)(k_{max}^3 - k_{max})\ \xi((\sinh \xi\ -\ \sin\ \xi)/(\cosh\ \xi + \cos\ \xi))$. The parameter $\xi = \pi\, d/2\delta$ is called the skin parameter and is proportional to the ratio of the wire diameter d to the skin depth δ.

IV. The core of EHQE-NMR theory

The *SNR* of EHQE-NMR is given by the ratio of signal Eq. S4 to the noise Eq. S6 and by inserting Eq. S8 for B_1/i,

$$SNR = \frac{|S_{max}|}{N} = \frac{\pi^{3/2}}{8\sqrt{k_B T}} \frac{Q_E}{(1 + R/R_E)} \frac{k_0 M_0 D_i^2 \mu_0}{\sqrt{L + L_E}} \left(n - \frac{n^2}{4W^2} + \frac{n^3}{24W^4} + O(n^4) \right) \quad \text{(S11)}.$$

Eqs. S9–S11 represent the core of the EHQE theory and allow a quantitative analysis of the *SNR*. The five basic properties of EHQE-NMR theory are: (a) The large *SNR* at low frequencies (1 kHz–10 MHz); (b) The initial linear increase in *SNR* with *n;* (c) The existence of a maximum SNR_{max} at the number of turns n_{max};

$$n_{max} = \left(\frac{3 L_E R_E}{2\pi \mu_0 \rho W^2} \right)^{1/3} \text{(S12)},$$

and (d) The hyperbolic decrease in *SNR* at large values of *n*. This latter decrease is caused mainly by the reduced enhancement factor $Q_{red} = Q_E/(1+R/R_E)$, which decreases with increasing *n* (Eq. S10). The final property is: (e) The weak dependence of the *SNR* on frequency $\omega/2\pi$ and on the sample volume *V*.

V. Experiments supporting EHQE-NMR theory

All of the aforementioned features described by Eqs. S9–S11 fully agree with the ^{1}H NMR measurements of benzene in Fig. 3 in the main text, where the *SNR* is plotted against *n* at five different frequencies $\omega/2\pi$ = 500, 166, 83.3, 41.6, and 20.8 kHz, respectively. The solid lines,

which represent EHQE theory, result from a plot of the calculated *SNR* according to Eqs. S9–S11 with the following measured fixed parameters: $D_i = H = 1$ cm, $W = 63$, $d = 0.12$ mm, ^{1}H polarization $P = 1.55 \times 10^{-6}$, ^{1}H spin number density $n_H = 2 \times 10^{22}$ /cm^3, sample volume $V = 450$ μL, and $Q_E = \{218,280,369,380,250\}$, $L_E = \{0.11, 0.55, 3.35, 18.2, 66\}$ mH, $R_E = \{1.7, 1.55, 4.8, 17.5, 34\}$ Ω at frequencies {500, 166, 83.3, 41.6, 20.8} kHz, respectively. The values for Q_E, L_E, and R_E were measured with an impedance spectrometer. The term L for the input coil is given by Eq. S9. The term R is determined by the value given by Eq. S10 and by an offset (~0.5–1 Ω) which is attributed to AC losses in the transfer line. Deviations in the experimental values of n_{max} from values predicted by Eq. S12 appear at 20–83 kHz in Fig. 3 (main text). To obtain exact values for n_{max} at low frequencies, Eq. S11 needs to be evaluated numerically with all nonlinear terms in n, searching for a maximum *SNR*.

VI. SNR comparison of EHQE-NMR to high-field NMR

The *SNR* for standard NMR in high field given by Eq. S2 can be compared directly to EHQE-NMR Eq. S11 provided that all nonlinear n terms in Eqs. S9–S11 are neglected. Assuming the same initial polarization P for a high-field and low-field EHQE-NMR experiment and neglecting proximity effects, the *SNR* in high field ($Q_{NMR} \sim 30$, $n_{NMR} \sim 3$, $L_{NMR} \sim 1$ nH at 500 MHz) is comparable to the *SNR* of EHQE-NMR at low field ($Q_{red} \sim 300$, $n \sim 90$, $L_{tot} = L + L_E \sim 0.1$ mH at 500 kHz) giving

$$\frac{SNR(\mathrm{EHQE}, 500\,\mathrm{kHz})}{SNR(\mathrm{NMR}, 500\,\mathrm{MHz})} = \frac{Q_{red}}{Q_{NMR}} \cdot \frac{n}{n_{NMR}} \cdot \sqrt{\frac{L_{NMR}}{L_{tot}}} \approx 1 \qquad (S13).$$

For $Q_{red} > 300$, the *SNR* of EHQE-NMR is expected to be better than standard high-field NMR.

VII. Predictions from EHQE-NMR theory

The model based on Eqs. S9–S11 is also useful for identifying the best possible SNR_{max} when more than one parameter changes. One example is demonstrated in Fig. S2, where the *SNR* is plotted as a function of the number of turns n and the wire diameter d at a frequency $\omega/2\pi$ = 500 kHz, and for Q_E = 314, $D_i = H$ = 1 cm. An absolute maximum SNR_{max} = 300 exists at n_{max} = 65 and d_{max} = 0.3 mm. For the slice in Fig. S2 with d = 0.12 mm, the maximum value is SNR_{max} = 190 at n_{max} = 75, which is close to the experimentally measured value for SNR_{max} at 500 kHz (see Fig. 3, main text).

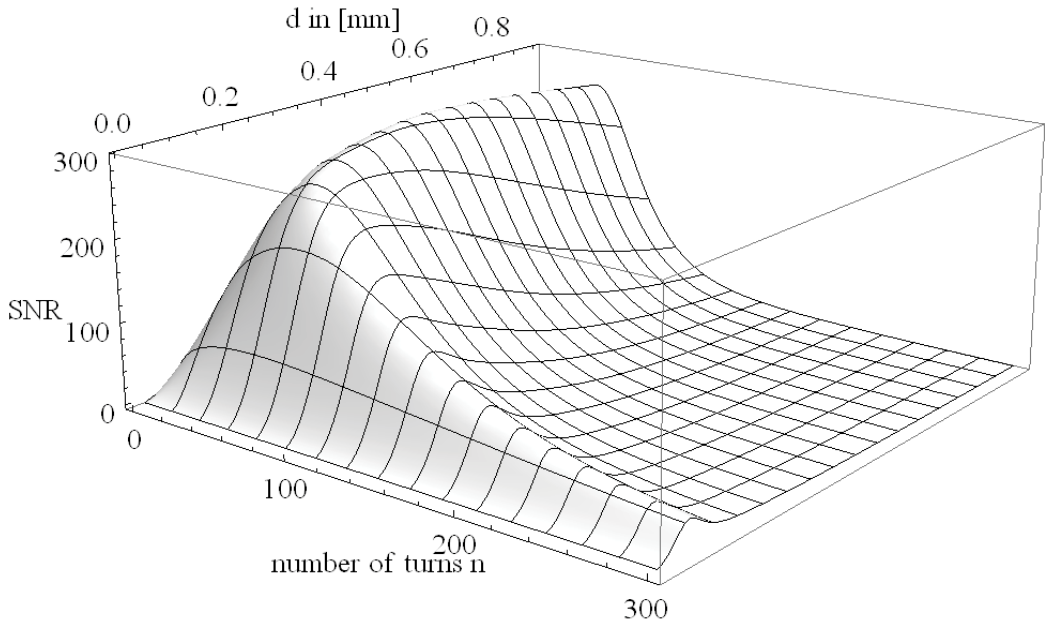

Fig. S2: *SNR* of EHQE ^{1}H NMR of 500 µL benzene as a function of the number of turns n and of the wire diameter d. The model parameters for Eqs. S7–S11 are $\omega/2\pi$= 500 kHz, Q_E = 314, L_E = 0.14 mH, R_E = 1.4 Ω , $D_i = H$ = 1 cm, and $P = 1.55 \cdot 10^{-6}$. The proximity effect is included. The maximum SNR_{max} = 300 is reached at n_{max} = 65 and d_{max} = 0.4 mm.

The analysis in Fig. S2 for determining the SNR_{max} in a two-parameter space $\{n, d\}$ can be repeated for other frequencies $\omega/2\pi$, keeping Q_E = 314 constant and adjusting L_{tot} at constant C to fulfil the resonance condition. This yields an n_{max} and a d_{max} for every SNR_{max} at every given frequency. Fig. S3 presents four different scenarios for SNR_{max} as a function of frequency (1 kHz – 10 MHz), keeping Q_E = 314 and $D_i = H$ = 1 cm constant. In all four

scenarios, the skin effect was included (see Eq. S10, section III) and n_{max} is determined by varying n. As a rule of thumb with increasing frequencies, n_{max} decreases, whereas d_{max} increases. In the first scenario (dotted line), the proximity effect is neglected ($Prox = 0$) and both n and d are optimized to obtain the corresponding SNR_{max}. Starting at $\omega/2\pi$ = 1kHz, the maximum signal to noise ratio first increases roughly with $SNR_{max} \sim \omega^{1/2}$ to a threshold at $\omega_{th} \sim 80$ kHz; then, $SNR_{max} = 300$ remains constant up to 10 MHz. The values of SNR_{max} below ~ 80 kHz are decreased because at lower frequencies, large numbers of turns n result in a large outer input coil diameter, leading to a reduced coil sensitivity B_1/i and to a higher DC resistance (which is nonlinear to n, see Eq. S10).

If the proximity effect is included (2nd scenario, dashed line), the SNR_{max} starts to drop below ~ 1 MHz until it reaches $SNR_{max} = 54$ at 1 kHz. In the kHz regime, there are many turns n and a large number of layers k_{max} in the input coil, leading to an exploding proximity effect $Prox \sim k_{max}^3$ (Eq. S10).

In the 3rd scenario (dash-dotted line), $Prox = 0$ and $d = 0.12$ mm are fixed. At $\omega/2\pi > 1$ MHz, the skin effect (skin depth $\delta \sim 0.065$mm @ 1MHz) becomes important at fixed $d = 0.12$ mm. At frequencies > 1 MHz, the skin depth δ decreases further and an increasing portion of the conductor with constant diameter becomes unutilized, and consequently SNR_{max} drops with increasing frequency. Between 10 kHz and 500 kHz, the SNR_{max} is rather flat, and close to 1 kHz, the SNR_{max} converges to the value of the 1st scenario. The 4th scenario (solid line) comes close to the real experiment by including the proximity and skin effects at a fixed $d = 0.12$ mm. Here, at low frequencies (10–500 kHz) SNR_{max} increases weakly with approximately $SNR_{max} \sim \omega^{0.14}$ (see Fig. 4a, main text) until it reaches a maximum at about 500 kHz. The experimental results (circles) are in good agreement with the theory (solid line). The slight deviations of the experimental data from the theoretical expectation results from

the variation of the measured Q_E values (218, 280, 369, 380, 250) around the value $Q_E = 314$ used for the theoretical prediction.

In future, further experiments will be needed in order to verify the predicted theoretical behaviour over a larger frequency range and at exact values of Q_E.

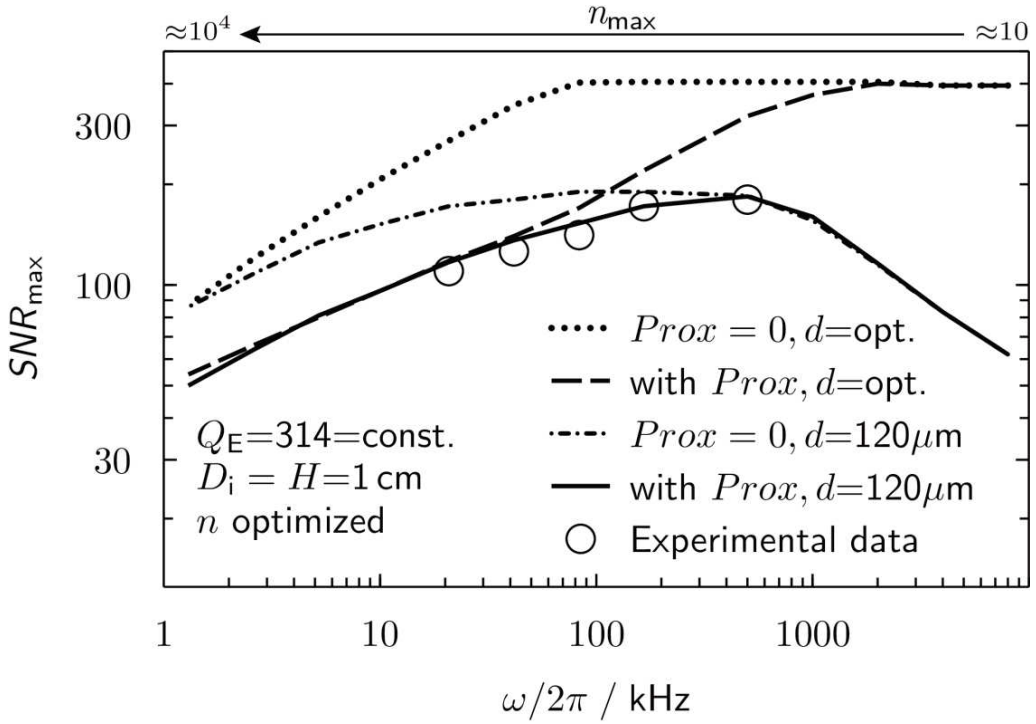

Fig. S3: Calculated maximum signal to noise ratio SNR_{max} of EHQE ^{1}H NMR of benzene ($P = 1.55 \cdot 10^{-6}$) as a function of frequency $\omega/2\pi$ (1 kHz–8 MHz) for constant $Q_E = 314$ and for $D_i = H = 1$ cm with optimized n. Dotted line: no proximity effect and wire diameter d optimized. Dash-dotted line: no proximity effect with constant $d = 0.12$ mm. Dashed line: with proximity effect and d optimized. Solid line: with proximity effect and constant $d = 0.12$ mm. Circles: experimental data.

Corresponding author: Stephan Appelt, e-mail: st.appelt@fz-juelich.de

References

[1] Abragam, A. *The Principles of Nuclear Magnetism* (Clarendon Press, Oxford, UK, 1961).

[2] Hoult, D. I., Richards, R. E. The signal-to noise ratio of nuclear resonance experiment. *Journal of Magnetic Resonance* **24**, 71-85 (1976).

[3] Ferreira, J. A., Improved Analytical Modeling of Conductive Losses in Magnetic Components. *IEEE Transactions on Power Electronics* **9**, 127–131 (1994).